Carbohydrate Polymers 144 (2016) 289–296

Contents lists available at ScienceDirect

Carbohydrate Polymers

journal homepage: www.elsevier.com/locate/carbpol

Impact of solvent quality on the network strength and structure of alginate gels

Elin Hermansson[a], Erich Schuster[b,c], Lars Lindgren[c,d], Annika Altskär[b,c], Anna Ström[a,c,*]

[a] Applied Chemistry, Chemistry and Chemical Engineering, Chalmers University of Technology, Gothenburg, Sweden
[b] Food and Bioscience, SP—Technical Research Institute of Sweden, Gothenburg, Sweden
[c] SuMo Biomaterials, VINN Excellence Center, Chalmers University of Technology, Gothenburg, Sweden
[d] Mölnlycke Health Care, P.O. Box 130 80, SE-40252, Sweden

ARTICLE INFO

Article history:
Received 25 November 2015
Received in revised form 18 February 2016
Accepted 22 February 2016
Available online 24 February 2016

Keywords:
Ethanol
Water–ethanol mixture
Small-angle X-ray scattering
Intrinsic viscosity
Hydrodynamic volume
Rheology

ABSTRACT

The influence of the mixture of water and alcohols on the solubility and properties of alginate and its calcium-induced gels is of interest for the food, wound care and pharmaceutical industries. The solvent quality of water with increasing amounts of ethanol (0–20%) on alginate was studied using intrinsic viscosity. The effect of ethanol addition on the rheological and mechanical properties of calcium alginate gels was determined. Small-angle X-ray scattering and transmission electron microscopy were used to study the network structure. It is shown that the addition of ethanol up to 15% (wt) increases the extension of the alginate chain, which correlates with increased moduli and stress being required to fracture the gels. The extension of the polymer chain is reduced at 20% (wt) ethanol, which is followed by reduced moduli and stress at breakage of the gels. The network structure of gels at high ethanol concentrations (24%) is characterized by thick and poorly connected network strands.

1. Introduction

Since the 1950s, hydrogel-based materials have been used for wound treatment. These materials provide a moist environment for the wound and promote different stages of wound healing. They are used in different forms, ranging from free-flowing gels with high water content and weak mechanical strength, to gel sheets with high material integrity (Lindholm, 2012). Polysaccharides such as alginate and hyaluronic acid are naturally abundant hydrophilic polymers suitable for hydrogel-based materials for wound care (Lloyd, Kennedy, Methacanon, Paterson, & Knill, 1998; Thomas, 2000).

Alginate is extensively used as a thickener and gelling agent in fields such as food (Draget, 2009; Ström et al., 2010) and pharmaceuticals (Lai, Abu'Khalil, & Craig, 2003; Rinaudo, 2008). The gels obtained from alginate are suitable for biomedical applications (Rinaudo, 2008) and as material for cell immobilization and signaling (Draget & Taylor, 2011; Lee & Mooney, 2012) owing to alginate's high biocompatibility, low cost and mild gelation process.

Alginate has a strong affinity for di- and trivalent cations, and rapidly forms a gel in the presence of low concentrations of such ions (Mg^{2+} being an exception) at a large range of pH values and temperatures. The polymer is mostly derived from brown algae but can also be produced by bacteria. It is a charged and linear copolymer consisting of (1-4)-linked β-D-mannuronic acid (M) and α-L-guluronic acid (G), whose ratio varies with the alginate source. The ability of alginate to form networks in the presence of divalent cations, where calcium has been specifically studied, is attributed to the chelation of calcium between G units from different alginate chains via the so-called egg-box model (Morris, Rees, Thom, & Boyd, 1978). The egg-box model involves a two-step network formation mechanism where the first step is a dimerization process followed by dimer–dimer aggregation of G units and Ca^{2+}, also referred to as junction zones.

The mechanical and rheological properties of calcium alginate gels depend on factors such as alginate type (Draget, Skjåk-Bræk, & Smidsrød, 1997; Skjåk-Bræk, Smidsrød, & Larsen, 1986), polymer and calcium concentrations (Mitchell & Blanshard, 1976; Stokke et al., 2000; Zhang, Daubert, & Foegeding, 2005), and introduction of calcium ions (Schuster et al., 2014; Stokke et al., 2000), as well as presence of monovalent ions (Seale, Morris, & Rees, 1982). In particular, the influence of calcium on alginate gel strength is well known, where increasing calcium at a fixed alginate concentration leads to an increased modulus (Mitchell & Blanshard, 1976; Zhang

* Corresponding author at: Department of Chemical and Biological Engineering, Chalmers University of Technology, 412 96 Gothenburg, Sweden.
E-mail address: anna.strom@chalmers.se (A. Ström).

http://dx.doi.org/10.1016/j.carbpol.2016.02.069

et al., 2005) until saturation (Schuster et al., 2014; Stokke et al., 2000), while the fracture strain is independent of both alginate and calcium concentrations (Zhang et al., 2005).

The influence of a mixture of water and non-aqueous solvents – for example, ethanol (EtOH) – on the ability of alginate to form calcium gels has, as far as we are aware, not been studied. Ethanol as a co-solute is interesting from a wound care perspective, primarily because of the antiseptic effect of this solvent, but it is also of interest for the food and beverage sector, as well as the pharmaceutical industry. In general, alcohols are used to decrease the solubility and to precipitate alginate, for example during extraction. The concentration of ethanol (in ethanol–water mixtures) required for 50% precipitation of the polymer has been studied and is dependent on the type of other ions present and their concentration in the mixture. An increasing concentration of mono- or di-valent ions lead to precipitation of alginate at lower ethanol concentrations (Smidsrød & Haug, 1967). Further, the influence of ethanol addition on the swelling of covalent crosslinked alginate beads has been determined. Moe, Skjåk-Bræk, Elgsaeter, and Smidsrød (1993) found a reduced swelling capacity of covalently cross-linked alginate beads in the presence of ethanol, which in addition is dependent on the type and concentration of monovalent ions. The onset of reduced swelling of the covalently cross-linked alginate beads is shifted to lower ethanol concentrations as the ionic strength of the monovalent salts NaCl and LiCl increases (Moe et al., 1993).

As outlined, the network formation and mechanical properties of calcium alginate gels have been extensively studied, but primarily in water as a pure solvent. In this paper, we report on the influence of ethanol as a co-solute on the physico-chemical properties (polymer size, network strength and structure) of alginate and calcium alginate gels at ethanol concentrations <24% (wt). We show that the intrinsic viscosity of alginate is increased at intermediate ethanol concentrations (10–15%) and that this increase correlates with increased shear moduli and stress at break of calcium alginate gels. The calcium alginate network structure, as determined by transmission electron microscopy (TEM) and small-angle X-ray diffraction (SAXS), does not appear to be affected by the addition of small amounts of EtOH. The network structure coarsens with increasing strand radii at intermediate EtOH concentrations.

2. Materials and methods

2.1. Materials

Alginate (Protanal RF 6650) was provided by FMC BioPolymer, Norway. It has a purity of 90% and the G-unit content is 65% according to the supplier. An elementary analysis was performed by Mikroanalytisches Laboratorium Kolbe, Germany, yielding the following mineral content of the alginate: calcium = 284 ppm, iron = 911 ppm, palladium = 305 ppm and cadmium = 71 ppm. Ethylenediaminetetraacetic acid (EDTA), sodium sulfate (Na_2SO_4) and D-glucono-δ-lactone (GDL) were purchased from Sigma–Aldrich, Sweden. Calcium carbonate ($CaCO_3$; Mikhart 2) was purchased from Provençale SA, France and had an average particle size of 10 mm. The ethanol used had a purity of 95% and was provided by Solveco, Sweden.

2.2. Methods

Alginate solutions (2% w/w) were prepared by careful addition of alginate powder to deionized water at room temperature under vigorous stirring. The dispersion was thereafter heated to 80 °C in a water bath and kept at this temperature for 30 min or until dissolution. The solution was cooled to room temperature before use. The pH of the polymeric solution was adjusted from pH 7.3 to pH 7 using 0.1 M hydrochlorid acid. Alginate gels were prepared by controlled release of calcium. $CaCO_3$ and GDL were rapidly dispersed in water and immediately added to the alginate solution to yield a final alginate concentration of 1% and calcium concentration of 1.2 mM and varying ethanol concentrations of 0, 8, 15 and 24%. The water required to dilute the alginate from 2 to 1% and in which the $CaCO_3$ and GDL was dispersed was reduced in order to accommodate the ethanol addition. The dispersions were poured into cylindrical Teflon molds (h = 12.5 mm; d = 12.5 mm) for large deformation testing. The molds were sealed and the samples were allowed to set and equilibrate at room temperature for 48 h prior to use. In the case of small deformation testing, the sample was loaded immediately onto the rheometer. It is important to note that the GDL was always used in stoichiometric equivalence to $CaCO_3$ (e.g., 15 mM $CaCO_3$ and 30 mM GDL) to keep the pH constant during network formation.

2.2.1. Oscillatory rheology

The rheological properties of the gels were determined using a Physica (MCR 300, from Anton Paar, Germany) with a cone and plate geometry. The cone has a diameter of 50 mm and an angle of 1° with a gap of 50 μm. The tests were performed at a fixed frequency of 6.3 $rads^{-1}$ and strain at 0.5%. To reduce evaporation, the measurements were performed in a closed atmosphere at T = 20 °C. The temperature was controlled by a Peltier system. The alginate/ethanol/$CaCO_3$ and GDL dispersion was quickly mixed and added subsequently to the rheometer (all in all, a time of approximately 30 s elapsed before the first measurement point was taken). The times at which G′ and G″ intersect were defined as gelling times.

2.2.2. Large deformation rheology

Uniaxial compression tests were performed on all gels using an Instron mechanical test frame (model 5565A). At least three repeats were done for each sample. The gel cylinders were carefully removed from the mold and aligned in the center of stainless steel compression plates, which were lubricated with mineral oil to reduce friction. Each gel was carefully examined for cracks or deformation resulting from handling prior to the testing. The samples were tested at room temperature with a maximum compression strain of 80% and a cross-head speed of 4% strain per second. True stress was calculated using Eq. (1):

$$\sigma = \frac{FH}{A_0 H_0} \tag{1}$$

and true strain was calculated from Eq. (2):

$$\gamma = \ln\frac{H}{H_0} \tag{2}$$

with F, H, A_0 and H_0 being the force used to compress the sample, the sample's height, the sample's initial area and the sample's initial height. The value of the stress at break was taken as the true stress that corresponded to the maximal obtained force.

2.2.3. Intrinsic viscosity

Alginate (0.5% w/w) was added to water at room temperature and dissolved at 80 °C for 30 min. The solution was thereafter transferred into dialysis membranes with a molecular weight cut-off size of 12–14 kDa. The solution was dialyzed against EDTA (0.01 M) for 2 days and against deionized water for the following 2 days. The dialysate was changed daily. The dialyzed material was freeze-dried for 2 days at −5 °C and a maximum of 1.65 mBar. The mineral content of the dialyzed material was analyzed by Mikroanalytisches Laboratorium Kolbe, Germany, yielding the following mineral content: calcium = 196 ppm, iron = 375 ppm, palladium = 68 ppm and cadmium = 16 ppm. The dialyzed and dried material was re-dissolved (0.5% w/w) in a Na_2SO_4 buffer (0.05 M). An automated

Ubbelohde viscometer (Schott-Geräte, Germany) with a capillary of 531 01a was used to determine the intrinsic viscosity of the alginate dispersed in buffer with increasing EtOH content. The capillary was immersed into a water-bath set at $T = 25\,^{\circ}C$. The average of flow-through time of solvent and dilute samples of alginate was determined for the calculation of relative and specific viscosity, η_{rel} and η_{spec}, respectively. The flow-through time of each sample was repeated 5 times. The Hagenbach corrections were applied to the running times before calculating the relative viscosity according to Eq. (3):

$$\eta_{rel} = \frac{\eta}{\eta_0} = \frac{t}{t_0} \tag{3}$$

where t equal corrected flow-through time and t_0 the corrected flow-through time of the solvent. The solvent is different for each series, that is, only buffer in the case of 0% EtOH, and appropriately added amount of EtOH to the buffer to achieve 5, 10, 12, 15 and 20% EtOH mixtures. The specific viscosity is given by Eq. (4):

$$\eta_{spec} = \frac{(\eta - \eta_0)}{\eta_0} = \eta_{rel} - 1 \tag{4}$$

The intrinsic viscosity, $[\eta]$ in dl/g, was determined by plotting η_{spec}/c and $\ln(\eta_{rel})/c$ against the concentration (c in g/dl) and extrapolating to zero concentration (Giannouli, Richardson, & Morris, 2004). The Huggins and Kraemer constants, k_H and k_K, respectively (sometimes also denoted as k' and k''), were determined from Eq. (5)

$$\frac{\eta_{spec}}{c} = [\eta] + k_H[\eta]^2 c \tag{5}$$

and Eq. (6) (Giannouli et al., 2004):

$$\frac{\ln \eta_{rel}}{c} = [\eta] + k_K[\eta]^2 c \tag{6}$$

The alginate concentrations chosen were varied for different ethanol concentrations in order to obtain a relative flow-through time (or relative viscosity, η_{rel}) smaller than 2.

2.2.4. Embedding and transmission electron microscopy

Small gel cubes, 1 mm × 1 mm × 1 mm, were cut out of the gel and fixed in 2% glutaraldehyde containing 0.1% Ruthenium Red in respective ethanol concentrations for each sample and calcium chloride ($CaCl_2$). The $CaCl_2$ concentration was chosen to correspond to the concentration of calcium at complete dissolution of the $CaCO_3$ used in the slow release system of $CaCO_3$ and GDL. During the embedding process, the alginate gel cubes were dehydrated in ascending series of ethanol and $CaCl_2$ solutions up to 99.5% ethanol, followed by 100% propylene oxide and ascending solutions of TAAB Low Viscosity Resin (TLV) at 2 concentrations up to the last step of pure TLV. The exchange of water during the dehydration step is performed gradually in order to minimize shrinkage; any shrinkage occurring is assumed to be isotropic and to not change the characteristics of the microstructure. The samples were embedded in epoxy resin TLV and polymerized for 20 h at 333 K. Ultrathin sections around 60 nm were cut with a diamond knife using an ultramicrotome (RMC Powertome XL, Boeckeler Instruments, USA). The ultrathin sections were placed on 400 mesh gold grids and stained with periodic acid, thiosemicarbazide and silver proteinate. Images of the alginate gel were recorded with a transmission electron microscopy LEO 706E (LEO Electron Microscopy Ltd., Germany), at 80 kV accelerating voltage.

2.2.5. Small-angle X-ray scattering

Small-angle X-ray scattering experiments were carried out using the I911-4 beamline at the MAX IV Laboratory in Lund, Sweden. An X-ray beam with a wavelength of 0.91 Å was selected. The SAXS patterns were collected using a Pilatus 1 M detector with a pixel size of 172 μm, which was located 1887 mm from the sample position, yielding a range of $q = 0.07–0.397\ nm^{-1}$. Scattering patterns were acquired at room temperature using exposure times of 30 s for solutions and 60 s for gelled samples. The data processing was carried out using Bli911-4 software. The alginate solutions were placed in a multiple-position sample holder (7.9 × 4 × 1.7 mm); the sample holder was sealed with Kapton tape on both sides. The alginate gels were prepared as described; directly before the measurement, they were cut in 4 × 4 × 1.7 mm blocks, placed in the multiple-position sample holder and sealed with Kapton tape. The contribution from scattering on the Kapton tape was subtracted from all data.

3. Results and discussion

3.1. Solution properties of alginate in EtOH–water mixtures

The intrinsic viscosity of a random coil such as alginate depends on the extension of the polymer coil. The "goodness" or the solvent quality of the solvents can thus be compared by determining the intrinsic viscosity of a polymer chain.

Experimental measurements of solution viscosity of dialyzed alginate dispersed in Na_2SO_4 (50 mM) with increasing amount of ethanol at $T = 25\,^{\circ}C$ were done within the range of $\eta_{rel} = 1.2–2.0$. Within this range, plots of η_{spec}/c and $\ln(\eta_{rel})/c$ against c (Huggins plot and Kraemer plot, respectively) should both be linear and extrapolate to a common intercept of $[\eta]$ as c approaches 0. Typical Huggins–Kraemer plots are shown in Fig. 1a. The $[\eta]$ plots thus obtained (Fig. 1b) show that the intrinsic viscosity of alginate goes through a maximum as EtOH is added between 0–24% (wt).

The obtained intrinsic viscosities at 0% ethanol concentration of 0.54 ml/mg is within the range of previously reported values, e.g., 0.52–1.44 ml/mg for different alginates obtained at 0.1 M NaCl and $T = 20\,^{\circ}C$ (Stokke et al., 2000). The molecular weight of the alginate can be calculated from the Mark–Houwink equation, $[\eta] = KM^a$. Using, $K = 4.85 \times 10^{-6}$ and $a = 0.97$ (Stokke et al., 2000), a molecular weight of 159 kDa is obtained for the alginate used here. The value of the molecular weight should however be treated with caution as both K and a are dependent of the ionic strength of the solvent (Smidsrød, 1970) and the given values of K and a are determined at 0.1 M NaCl while the intrinsic viscosity in this study was determined an ionic strength of 50 mM Na_2SO_4.

As indicated in Fig. 1b, the intrinsic viscosity is higher at an EtOH concentration of 10–15% than at concentrations of 0% and 5%. At an EtOH concentration of >15%, the intrinsic viscosity decreases sharply. Increased intrinsic viscosity indicates that the alginate chain occupies an increased volume, equivalent to an increased hydrodynamic volume and a more extended polymer chain. The reduction in hydrodynamic volume at higher ethanol concentrations clearly shows that an increased ethanol concentration is a poor solvent for the negatively charged alginate. Smidsrød and Haug (1967) have shown that precipitation of alginate (in the presence of 50 mM NaCl) occurs at an ethanol concentration of 40%. The tendency of alginate chains to contract at a considerably lower EtOH concentration than 40% could be related to the more precise methodology used in this study. It is expected that impact on the polymer chain is revealed at a lower concentration than the actual precipitation. It is worthwhile to note that no increase in turbidity was observed visually for the ethanol concentrations used in this study, indicating the absence of large polymer aggregates.

Graphical assessment of the intrinsic viscosity allows for the determination of the Huggins constant, k_H, and the Kraemer constant, k_K via Eqs. (5) and (6). Generally, higher affinity between polymer and solvent result in lower values of k_H (Delpech & Oliveira, 2005; O'sullivan, Murray, Flynn, & Norton, 2016). Negative

Table 1
The intercept obtained upon extrapolating the Kraemer and Huggins plots to zero concentration, intrinsic viscosity ([η]), the Huggins constant (k_H) and Kraemer constant (k_H) as well as the difference between k_H and k_K for alginate solutions in 50 mM buffer at different EtOH concentrations and T = 25 °C.

EtOH conc./%	Intercept based on Huggins plot	Intercept based on Kraemer plot	[η]/ml mg^{-1}	k_H	k_K	$\Delta k = k_H - k_K$
0	0.54	0.53	0.54	0.45	−0.10	0.55
5	0.53	0.53	0.53	0.58	−0.01	0.59
10	0.61	0.61	0.61	0.39	−0.13	0.52
12	0.72	0.70	0.71	0.01	−0.34	0.35
15	0.60	0.60	0.60	0.13	−0.31	0.44
20	0.21	0.22	0.22	18	14	32

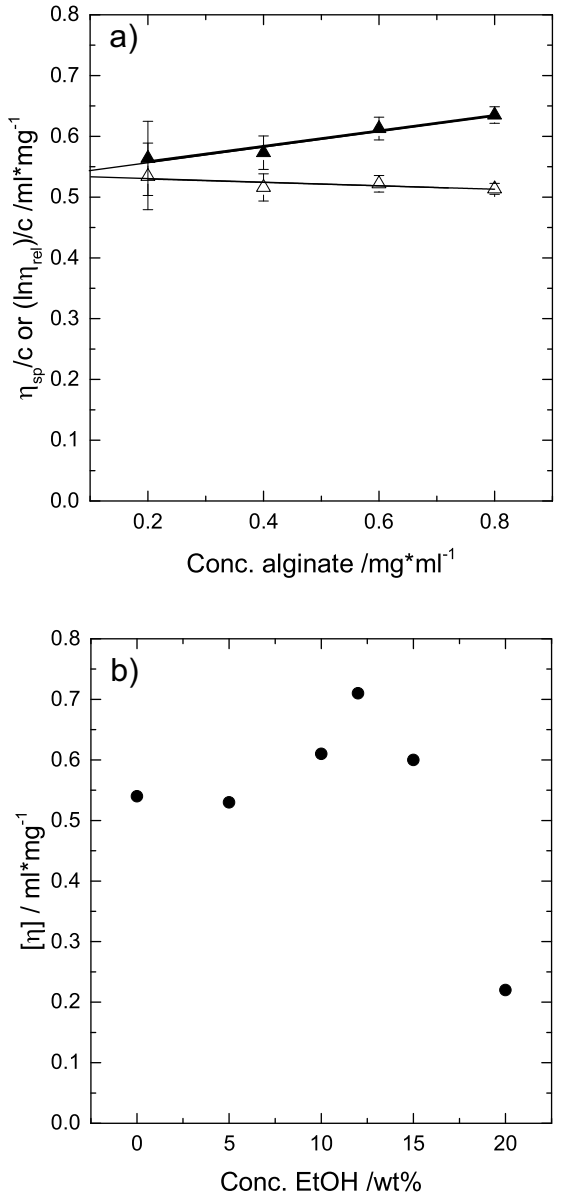

Fig. 1. (a) Huggins and Kraemer plots constructed for the determination of intrinsic viscosity of alginate. Huggins (η_{spec}/c) [filled symbols] and ln(η_{rel})/c [open symbols] against the concentration of alginate in 50 mM Na_2SO_4 buffer, and (b) [η] obtained via Huggins and Kraemer plots for different EtOH–water mixtures. All measurements performed at T = 25 °C. The error bars correspond in (a) to standard deviations from 4 runs.

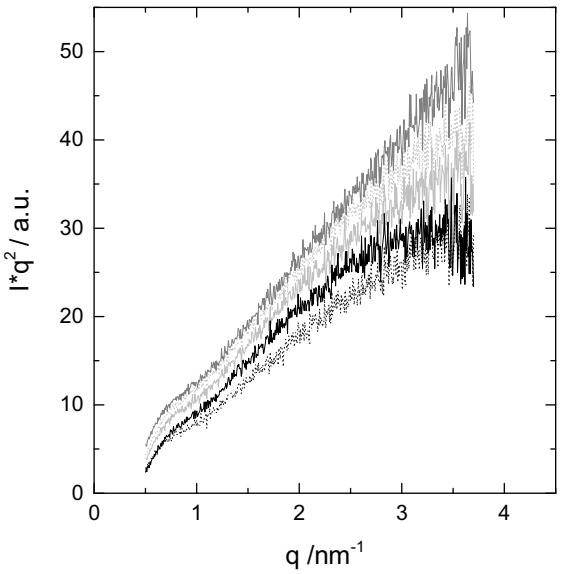

Fig. 2. SAXS data of alginate solutions in water with increasing ethanol addition, 0% ethanol (black), 5% (dotted black), 10% (grey), 15% (dotted grey) and 24% (dark grey), presented as a Kratky plot.

values of k_K are attributed to good solvation while positive values of k_K to poor solvent (Delpech & Oliveira, 2005; O'sullivan et al., 2016). k_H for non-associating rod-like macromolecules lay within the range 0.4–0.7, where alginate in NaCl solutions of 0.005–0.2 M yield values of k_H between 0.35–0.55. The values of k_H obtained in this study (Table 1) for EtOH concentrations of 10% are close to the previously reported values for alginate in NaCl solution and or non-associating rod-like macromolecules (Delpech & Oliveira, 2005). At higher EtOH concentration (12 and 15%), k_H reduces below 0.35. k_K is negative for all tested samples with EtOH ≤ 15% (Table 1), indicating good solvation. In contrast, the high positive values of both k_H and k_K show poor solvation of alginate in 20% EtOH. Increase in intrinsic viscosity and reducing values of k_H were observed also for gelatin in water–alcohol mixtures (Bohidar & Rawat, 2014).

The difference between k_H and k_K should theoretically be 0.5, this relation is fulfilled in the case of 0% EtOH and 10% EtOH but not for the other samples tested. Deviation from $k_H - k_K = 0.5$ is known to occur for proteins and amphiphilic polymers (O'sullivan et al., 2016), aggregating polymers (Delpech & Oliveira, 2005) as well as gelatin in water–alcohol mixtures (Bohidar & Rawat, 2014).

While we expected that increasing amounts of ethanol would result in a poorer solvent for alginate, we did not expect that a small amount of added ethanol would lead to a more extended polymer chain at ethanol concentrations of 10–15%. Small-angle X-ray scattering of alginate solutions in water–ethanol mixtures (Fig. 2) further confirmed the stiffening of the alginate chain upon addition of EtOH (as shown via intrinsic viscosity measurements). The Kratky plot of the alginate solution without EtOH (black line in Fig. 2) starts plateauing at high q-values and indicates that the alginate chain is flexible and has the characteristics of a Gaussian chain. The plateau disappears for the alginate solutions with added EtOH and a Kratky plot increases linearly at high q-values. This scaling resembles stiff rods and indicates that the alginate chains are stiffer in the presence of ethanol.

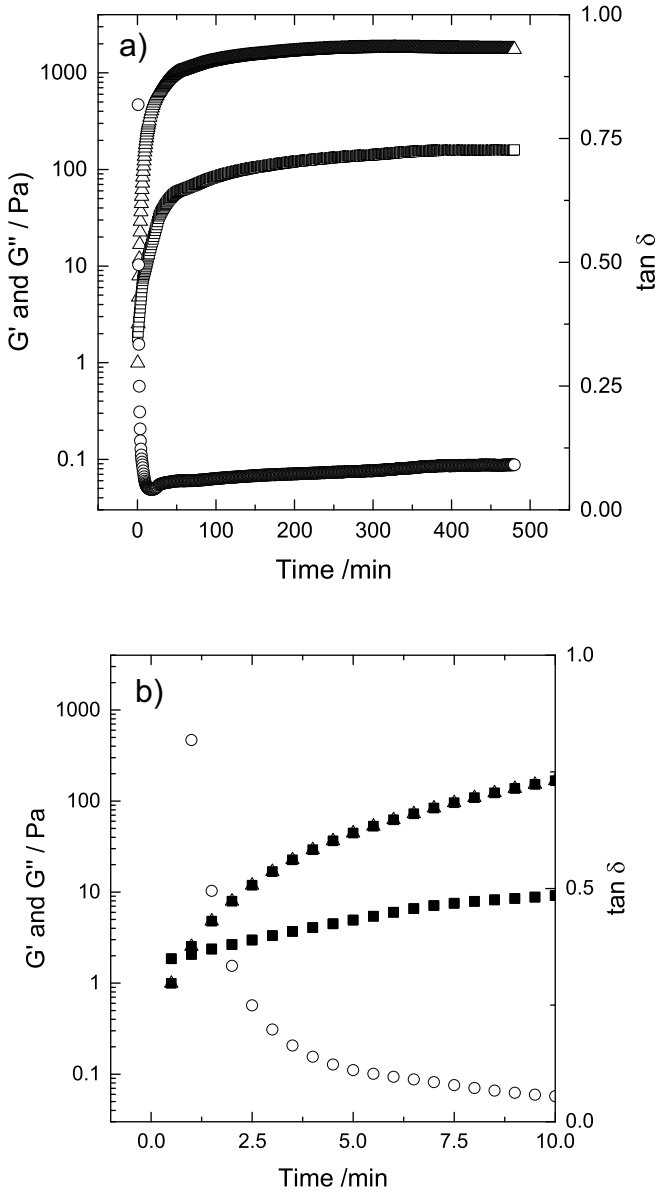

Fig. 3. Time evolution of G′ (triangles), G″ (square) and tan δ (circle) at an angular frequency of 6.28 rad/s and at a fixed strain of 0.5% of 1% alginate with a calcium concentration fixed at 1.2 mM as a function of time: (a) 0–500 min and (b) 0–10 min.

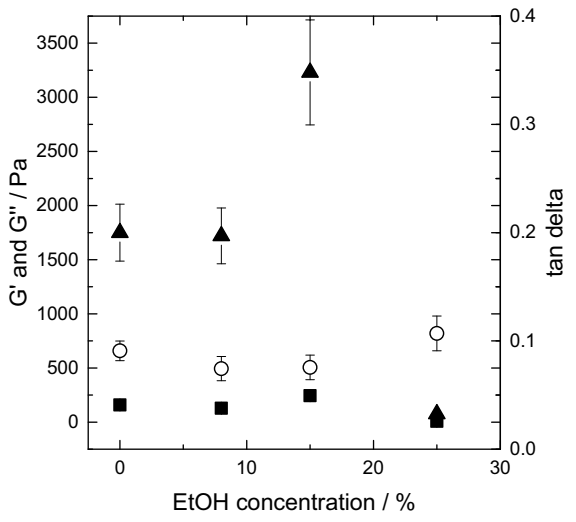

Fig. 4. The influence of ethanol concentration on G′ (triangle), G″ (square) and tan δ (circle) of calcium alginate gels at 1% alginate and calcium concentration of 1.2 mM. Measured at an angular frequency of insert number rad/s and at a fixed strain of 0.5% and $T = 20\,^{\circ}C$.

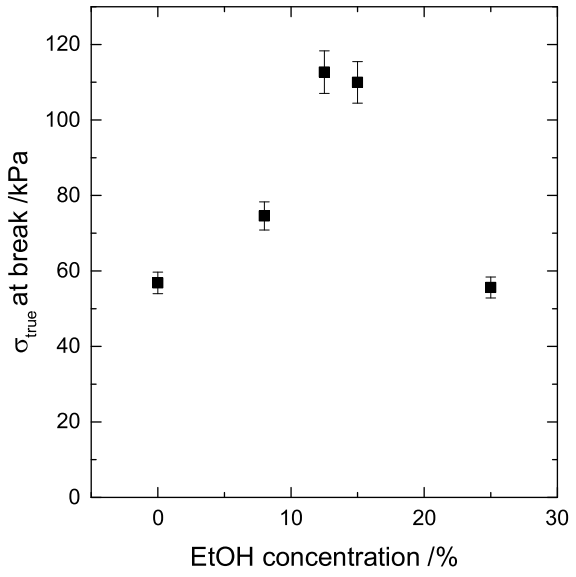

Fig. 5. True stress at break of calcium alginate gels in ethanol water mixtures. All samples were tested at room temperature with 1% alginate and 1.2 mM Ca^{2+} after 24 h of curing. Five gels were tested for each composition.

3.2. Rheological properties of calcium alginate in EtOH–water mixtures

The influence of ethanol addition on gelation and gel strength of calcium alginate gels was studied by small and large deformation rheology. The gelation was induced by the addition of a $CaCO_3$/GDL system that allowed for a slow release of calcium and thus controlled internal setting of calcium alginate gels (Ström & Williams, 2003). Fig. 3a shows the time evolution of the storage (G′) and the loss (G″) moduli upon the addition of $CaCO_3$/GDL. Note that $CaCO_3$/GDL was added shortly before loading to the rheometer (we estimated that it took 2 min from the addition of $CaCO_3$/GDL, the mixing, the loading and the start-up of the instrument, to the first measurement point). As expected, the crossover of G′ and G″ (G > G″) occurs within minutes (Fig. 3b), indicating the formation of a gel. The gel strength increases rapidly during the first 50 min, and then levels out and equilibrates at times >100 min. The time evolution of gels is similar for the cases of calcium alginate gelation in 0–15% of ethanol. A more rapid initial gelation and gel growth is observed in the case of ethanol concentrations of 24%. It should be noted that alginate in ethanol–water mixtures appears perfectly transparent, giving no indication of large-scale aggregates; likewise, the gel containing 24% ethanol appears transparent once the $CaCO_3$ is fully dissolved.

Plotting the storage and loss moduli obtained at time = 480 min as a function of ethanol concentration (Fig. 4) reveals a similar trend as for the intrinsic viscosity—that is, no change in G′ and G″ is observed between 0% and 10% EtOH, but increased moduli are observed at 15%, followed by a sharp reduction at 24% EtOH. The value of tan δ (tan δ = G″/G′) did not vary much between the samples (reduced from 0.1 to 0.08 upon addition of ethanol to increase again to 0.11 at the highest amount of EtOH).

The stress at break and the strain at break of gels with fixed calcium and alginate concentration but increasing EtOH concentration were further tested (Fig. 5). Again, the stress at break follows a similar dependence on the EtOH concentration as the intrinsic

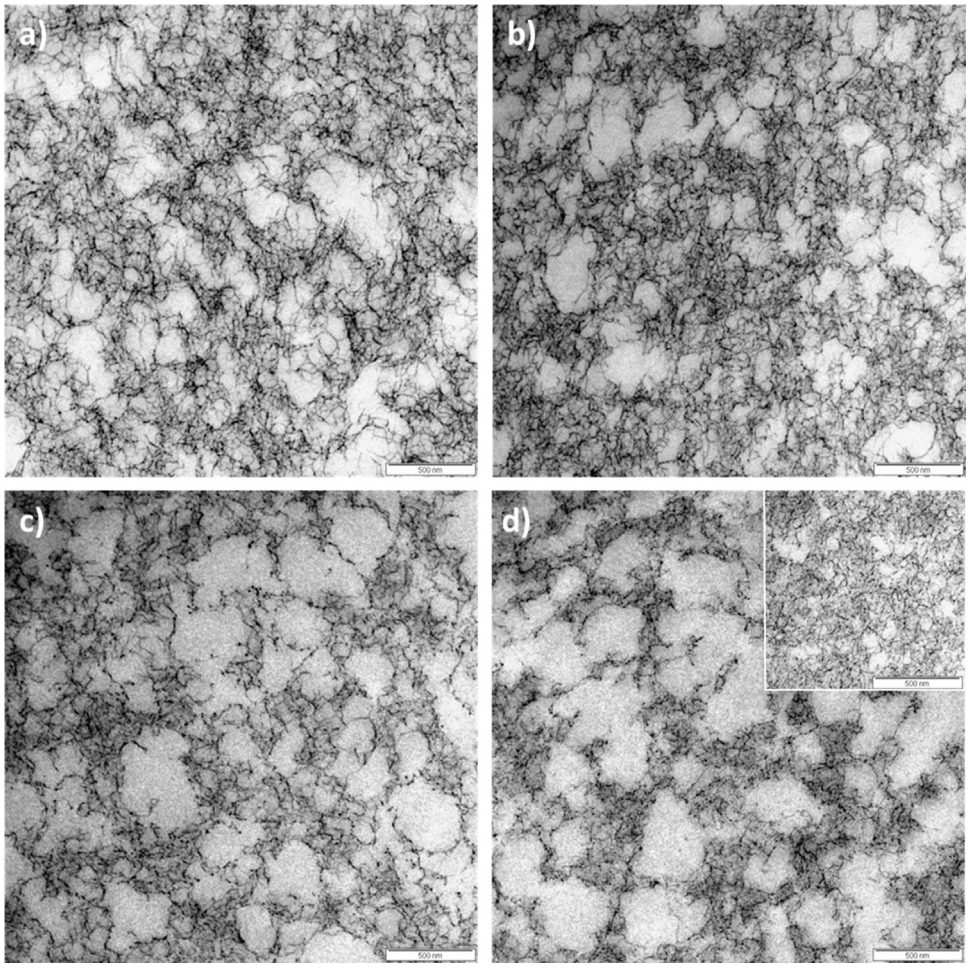

Fig. 6. TEM images of calcium alginate gels in the presence of (a) 0%, (b) 8%, (c) 15% and (d) 24% ethanol. The scale bar represent 500 nm.

viscosity and the moduli. A maximum is observed at EtOH values around 15%, followed by a drastic reduction in stress at break at the highest tested EtOH concentration.

Both small and large deformation results show that a moderate amount of ethanol (here 15%) promotes the strength of the gel network, while a higher ethanol concentration of 24% reduces the strength. Similarly, small amount of methanol, <6% have shown to promote and increase the network strength of HM pectin, while 10% addition of methanol reduces the gel strength (Tho, Kjøniksen, Nyström, & Roots, 2003). An increase in elastic modulus corresponds to a more extended and stiffer polymer chain, and the drop in elastic and viscous moduli corresponds to a less extended polymer chain.

In the case of fully cured physical gels, the moduli are, as in rubber theory, proportional to the number of elastically active network chains (EANCs) and RT, which is a measure of the average contribution per mole of EANCs to the free energy increase per unit strain to G (Clark, 1994). In other words, networks composed of biopolymers have stress-bearing filaments or EANCs of certain stiffness. Such stress-bearing filaments contribute to the overall increase in free energy owing to the deformation (Clark, 1994; Storm, Pastore, MacKintosh, Lubensky, & Janmey, 2005), and are well described within the framework of semi-flexible polymer physics and can, for example, be treated by a wormlike-chain model (Kroy & Frey, 1996). In this study, both the calcium and the polymer concentrations are the same. Unless the more extended chains open up to expose otherwise hidden guluronate groups that can bind calcium, we can assume no more junction zones are created. As the concentration of calcium used in this study is not high enough to saturate the potential binding sites (even before polymer chain extension)—that is, the alginate contains more calcium chelating guluronate units than added calcium (ratio of $2 \times [Ca^{2+}]$:[guluronate] equals 0.75)—the assumption that more junction zones are not created appears valid.

Furthermore, the number of available alginate chains remains constant. That would mean that the increased moduli are related to an increased stiffness of the network-constituting elements. The force extension relationship of a semi-flexible chain does describe this phenomenon: the more extended the chain becomes, the higher the force needed to keep it at this extension (and it increases mostly in a non-linear fashion). This also means that more extended chains contribute more to the network stiffness and thus cause a higher modulus (Schuster, Lundin, & Williams, 2012; Storm et al., 2005). It is interesting to note the correlation between the behavior of a single polymer chain (in this study determined via intrinsic viscosity) and macroscopic behavior such as bulk rheology. Free energy calculations on guluronic acid chains similarly indicated a deviation from rubber elasticity, due to the stiffening of the polymer for short end-to-end distances of the polymer (Bailey, Mitchell, & Blanshard, 1977). A link between single polymer chain behavior and bulk functionality was also observed in the study of Moe et al. (1993) where they correlate the behavior of alginate in solution and the swelling of covalently cross-linked alginate beads.

Increased stress at break (large deformation) of alginate gels has been correlated with the junction zones themselves, rather than with the polymer segments between the junction zones (Zhang

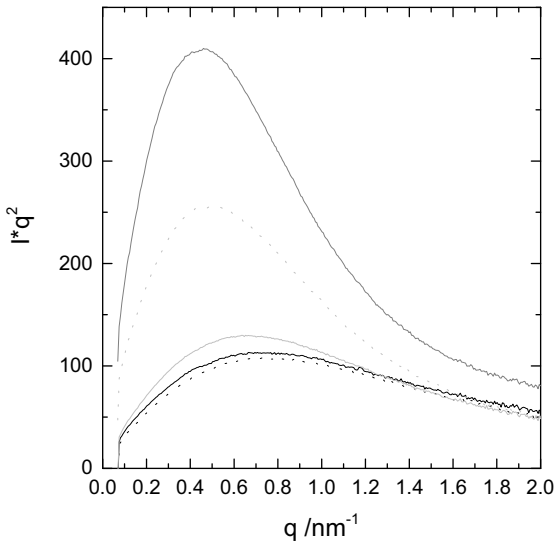

Fig. 7. SAXS data of the calcium alginate gels with increasing ethanol concentration, 0% (black), 5% (dotted black), 10% (grey), 15% (dotted grey) and 24% dark grey, presented as a Kratky plot.

et al., 2005), as is common in small deformation. Increased stress at break at 15% EtOH could therefore be related to more loadbearing junctions, thus distributing the compressive force over more junctions and resulting in the ability of the gel to support an overall higher force. Alternatively, the increased stress at break could be related to the gel with 15% EtOH having junction zones that are stronger—for example, via increased lateral aggregation of the junctions. Next section will show that increased lateral aggregation of the junctions appears a likely explanation to the observed increase in fracture strength.

3.3. Network structure of calcium alginate in EtOH–water mixtures

The local network structure of the calcium alginate gels formed in the presence of EtOH was studied with TEM and SAXS. The TEM images of the calcium alginate gels formed in the presence of increasing amount of EtOH are shown in Fig. 6. The network structure of the calcium alginate formed in absence of EtOH (Fig. 6a) is characterized by an overall homogeneous structure, similarly to what would be expected (Bernin et al., 2011; Schuster et al., 2014). The addition of small amount of EtOH (8%) does not alter the overall network structure (Fig. 6b). The alginate gels with 15% and 24% ethanol have a different microstructure compared to the previous two. The gel microstructure appears more heterogeneous, with a denser, more compact network of polymer strands and the pores appearing larger and more rounded in the case of 15% EtOH (Fig. 6c) than in the samples containing 0% and 8% ethanol. In the alginate gel with 24% ethanol (Fig. 6d), we see an even more compact polymer network with larger pores than the other alginate gels (0%, 8% and 15%). The polymer network appears less connected and areas where the polymer appears precipitated are observed (insert 6d).

The SAXS data on the alginate gels (Fig. 7) correspond well with the TEM microstructures. All Kratky plots show a maximum in the recorded q-range. This scaling corresponds to the scatter of a branched system (mass fractal), in contrast to the stiff rods and Gaussian chains discussed in Section 3.1. The observed changes between the SAXS data on the alginate solutions can be explained by the buildup of an interconnected gel network structure. The Kratky plot of the SAXS data on calcium alginate gels in the absence of EtOH shows a maximum at $q = 0.75\ \mathrm{nm}^{-1}$. The maximum of the Kratky plot is shifted to smaller q-values upon increased ethanol content for samples with >5% EtOH. A shift of the Kratky plot toward smaller q-values has been attributed to the lateral association of junctions with larger dimensions and cross-sectional radii (Stokke et al., 2000). Additionally, the scattering profile was analyzed in the q-range of the Guinier regime. This analysis revealed cross-sectional radii of gyration for the different ethanol concentrations of $R_c = 1.47$ nm (0% EtOH), $R_c = 1.47$ nm (5% EtOH), $R_c = 1.60$ nm (10% EtOH), $R_c = 1.98$ nm (15% EtOH) and $R_c = 2.11$ nm (24% EtOH), confirming an increase in network bundle size for higher ethanol concentrations.

The SAXS data confirms the network impression obtained by TEM: denser network clusters are formed at higher EtOH concentrations.

Correlating the microstructure of physical networks with their rheological properties (small deformation) appears difficult. Stokke et al. (2000) specifically looked for similar local structures (using SAXS) of calcium alginate gels with similar rheological properties but different calcium concentrations and alginate types. The scattering profiles of the gels were different, suggesting that local structures and rheological properties of gels can be varied independently (Stokke et al., 2000). Furthermore, the morphology of many physical gels (pectin, alginate and carrageenan) appears similar, even though gelation mechanism and small deformation rheology properties differ (Hermansson, 2008). For example, pectin networks did not show a difference in morphology as visualized using TEM, while their rheology was different (Löfgren, Guillotin, & Hermansson, 2006). It has been speculated that the interaction between the strands and their connectivity is difficult to assess from TEM images, which could be a reason for the difficulty to correlate rheological function to microstructure of alginate gels (Schuster et al., 2014).

In this study, we explain the small deformation properties of the calcium alginate gels via an approach inspired by rubber theory (Clark, 1994; Schuster et al., 2012; Storm et al., 2005) and observe similarities in the single alginate chain properties and small deformation rheology of the calcium alginate gels upon the addition of EtOH. It is however difficult to explain the small deformation behavior with SAXS or TEM images, in agreement with above mentioned studies. The large deformation properties of calcium alginate gels have been proposed to be governed by strengthening of junctions via lateral aggregation (Zhang et al., 2005). In this case, both visual impression from TEM images and SAXS data support an increased aggregation of junctions, explaining the increased stress required to break the gel at 15% EtOH (Fig. 5). The TEM images reveal the onset of precipitation of the polymer and poorly connected network at 24% EtOH concentration explaining why reduced stress is required to break the calcium alginate gel at 24% EtOH despite increased strand radii as determined by SAXS. The study show the importance of obtaining complementary information obtained via TEM and SAXS but also single polymer physics in order to understand rheological and mechanical properties of physical networks.

4. Conclusions

We show in this study that the addition of low to moderate (up to 15%) concentrations of ethanol increases the intrinsic viscosity (extension) of alginate. The solvent quality is reduced at higher ethanol concentrations (20%) as reflected by a reduced intrinsic viscosity.

Both the moduli and the stress at break show the same trend as the intrinsic viscosity. The moduli and the stress at break reach a maximum upon the addition of ethanol of 15%, after which they reduce. It is expected that a more extended and stiffer polymer chain contributes more to the network stiffness (the modulus) than a less extended polymer chain does. The behavior of single polymer

chains, obtained via intrinsic viscosity measurements, correlates here nicely with the rheological and mechanical properties of the bulk network at a fixed calcium concentration.

SAXS data and visual impressions obtained by TEM correlate well and indicate a coarsening of network strands and an increasingly heterogeneous network at moderate (15%) to high (24%) ethanol concentrations. It is possible that the increased stress at break observed at 15% EtOH is related to the increase in network bundle size. For the sample containing 24% EtOH, the network bundle size is large but the TEM images show regions of partly precipitated polymer and a poorly connected network contributing to the weakening of the gel.

Acknowledgements

The financial contribution from the VINN Excellence Center's SuMo BIOMATERIALS and Vinnmer program from VINNOVA for A.S is acknowledged. As well, we thank Tomas Fabo for initiating the project and for interesting discussions. We also thank the MAX IV Laboratory for use of the MAX II SAXS beamline I911-SAXS.

References

Bailey, E., Mitchell, J. R., & Blanshard, J. M. V. (1977). Free energy calculations on stiff chain constituents of polysaccharide gels. *Colloid and Polymer Science*, *255*(9), 856–860.

Bernin, D., Goudappel, G. J., van Ruijven, M., Altskar, A., Ström, A., Rudemo, M., et al. (2011). Microstructure of polymer hydrogels studied by pulsed field gradient NMR diffusion and TEM methods. *Soft Matter*, *7*, 5711–5716.

Bohidar, H. B., & Rawat, K. (2014). Biological polyelectrolytes: solutions, gels, intermolecular complexes and nanoparticles. In P. M. Vishak, O. Bayraktar, & G. A. Picó (Eds.), *Polyelectrolytes, thermodynamics and rheology* (pp. 113–182). Springer.

Clark, A. H. (1994). Rationalisation of the elastic modulus-molecular weight relationship for kappa-carrageenan gels using cascade theory. *Carbohydrate Polymers*, *23*, 247–251.

Delpech, M. C., & Oliveira, C. M. F. (2005). Viscometric study of poly(methyl methacrylate-*g*-propylene oxide) and respective homopolymers. *Polymer Testing*, *24*, 381–386.

Draget, K. (2009). Alginates. In G. O. Phillips, & P. A. Williams (Eds.), *Handbook of hydrocolloids* (2nd ed., pp. 807–828). London, UK: Elsevier Applied Science.

Draget, K. I., & Taylor, C. (2011). Chemical: physical and biological properties of alginates and their biomedical implications. *Food Hydrocolloids*, *25*, 251–256.

Draget, K. I., Skjåk-Bræk, G., & Smidsrød, O. (1997). Alginate based new materials. *International Journal of Biological Macromolecules*, *21*, 47–55.

Giannouli, P., Richardson, R. K., & Morris, E. R. (2004). Effect of polymeric cosolutes on calcium pectinate gelation. Part 1. Galactomannans in comparison with partially depolymerised starches. *Carbohydrate Polymers*, *55*, 343–355.

Hermansson, A. M. (2008). Chapter 13. Structuring water by gelation. In J. Aguilera, & P. Lillford (Eds.), *Food materials science: principles and practice* (pp. 255–280). Springer Verlag.

Kroy, K., & Frey, E. (1996). Force-extension relation and plateau modulus for wormlike chains. *Physical Review Letters*, *77*, 306.

Lai, H. L., Abu'Khalil, A., & Craig, D. Q. (2003). The preparation and characterisation of drug-loaded alginate and alginate sponges. *International Journal of Pharmaceutics*, *251*, 175–181.

Lee, K. Y., & Mooney, D. J. (2012). Alginate: properties and biomedical applications. *Progress in Polymer Science*, *37*, 106–126.

Lindholm, C. (2012). *Sår* (3rd ed.). Studentlitteratur AB. ISBN 978-91-44-05442-1.

Lloyd, L. L., Kennedy, J. F., Methacanon, P., Paterson, M., & Knill, C. J. (1998). Carbohydrate polymers as wound management aids. *Carbohydrate Polymers*, *37*, 315–322.

Löfgren, C., Guillotin, S., & Hermansson, A.-M. (2006). Microstructure and kinetic rheological behavior of amidated and nonamidated LM pectin gels. *Biomacromolecules*, *7*, 114–121.

Mitchell, J., & Blanshard, J. (1976). Rheological properties of alginate gels. *Journal of Texture Studies*, *7*, 219–234.

Moe, S. T., Skjåk-Bræk, G., Elgsaeter, A., & Smidsrød, O. (1993). Swelling of covalently crosslinked alginate gels: influence of ionic solutes and nonpolar solvents. *Macromolecules*, *26*, 3589–3597.

Morris, E. R., Rees, D. A., Thom, D., & Boyd, J. (1978). Chiroptical and stoichiometric evidence of a specific: primary dimerisation process in alginate gelation. *Carbohydrate Research*, *66*, 145–154.

O'sullivan, J. O., Murray, B., Flynn, C., & Norton, I. (2016). The effect of ultrasound treatment on the structural, physical and emulsifying properties of animal and vegetable proteins. *Food Hydrocolloids*, *53*, 141–154.

Rinaudo, M. (2008). Main properties and current applications of some polysaccharides as biomaterials [review]. *Polymer International*, *57*, 397–430.

Schuster, E., Lundin, L., & Williams, M. A. (2012). Investigating the relationship between network mechanics and single-chain extension using biomimetic polysaccharide gels. *Macromolecules*, *45*, 4863–4869.

Schuster, E., Eckardt, J., Hermansson, A.-M., Larsson, A., Lorén, N., Altskär, A., et al. (2014). Microstructural, mechanical and mass transport properties of isotropic and capillary alginate gels. *Soft Matter*, *10*, 357–366.

Seale, R., Morris, E. R., & Rees, D. A. (1982). Interactions of alginates with univalent cations. *Carbohydrate Research*, *110*, 101–112.

Skjåk-Bræk, G., Smidsrød, O., & Larsen, B. (1986). Tailoring of alginates by enzymatic modification *in-vitro*. *International Journal of Biological Macromolecules*, *8*, 330.

Smidsrød, O. (1970). Solution properties of alginate. *Carbohydrate Research*, *13*, 359–372.

Smidsrød, O., & Haug, A. (1967). Precipitation of acidic polysaccharides by salts in ethanol–water mixtures. *Journal of Polymer Science: Part C*, *16*, 1587–1598.

Stokke, B. T., Draget, K. I., Smidsrød, O., Yuguchi, Y., Urakawa, H., & Kajiwara, K. (2000). Small-angle X-ray scattering and rheological characterisation of alginate gels. 1. Ca-alginate gels. *Macromolecules*, *33*, 1853–1863.

Ström, A., & Williams, M. A. (2003). Controlled calcium release in the absence and presence of an ion-binding polyme. *Journal of Physical Chemistry B*, *107*, 10995–10999.

Storm, C., Pastore, J. J., MacKintosh, F. C., Lubensky, T. C., & Janmey, P. A. (2005). Nonlinear elasticity in biological gels. *Nature*, *435*, 191–194.

Ström, A., Melnikov, S., Koppert, R., Boers, H. M., Peters, H. P. F., Schuring, E. A. H., et al. (2010). Physico-chemical properties of hydrocolloids determine its appetite effects. In P. A. Williams, & G. O. Phillips (Eds.), *Gums and stabiliser for the food industry 15*. Royal Society of Chemistry (RSC).

Tho, I., Kjøniksen, A. L., Nyström, B., & Roots, J. (2003). Characterization of association and gelation of pectin in methanol–water mixtures. *Biomacromolecules*, *4*, 1623–1629.

Thomas, S. J. (2000). Alginate dressings in surgery and wound management—Part 1. *Wound Care*, *9*, 56–60.

Zhang, J., Daubert, C. R., & Foegeding, E. A. (2005). Fracture analysis of alginate gels. *Journal of Food Science*, *70*, E425–E431.